International Journal of Nanoelectronics and Materials

In Press, Accepted Manuscript – Note to user

Annealing Effects on Polycrystalline Silicon Germanium (SiGe) Thin Films grown on Nanostructured Silicon Substrates using Thermal Evaporation Technique.

Azhari, A. W.[1,2*], Eop, T. S.[1,2], Che Halin, D. S. [3], Sopian, K. [4], Hashim, U. [5], Zaidi, S. H. [6]

[1]Faculty of Civil Engineering Technology, Universiti Malaysia Perlis (UniMAP), Kangar, Perlis, Malaysia
[2]Centre of Excellence, Water Research and Environmental Sustainability Growth, (WAREG), Universiti Malaysia Perlis (UniMAP), Perlis, Malaysia
[3]Center of Excellence, Geopolymer and Green Technology (CEGeoGTech), Universiti Malaysia Perlis (UniMAP), Kangar Perlis, Malaysia
[4]Solar Energy Research Institute (SERI), Universiti Kebangsaan Malaysia (UKM), Bangi, Selangor, Malaysia
[5]Institute of Nano Electronic Engineering (INEE), Universiti Malaysia Perlis (UniMAP), Kangar, Perlis, Malaysia
[6]Gratings Incorporated Albuquerque, USA

Received 22 September 2021, Revised 8 March 2022, Accepted 22 June2022

ABSTRACT

Polycrystalline SiGe thin films have been formed after thermal annealing of formerly vacuum evaporated a-Ge layers. The a-Ge thin films were deposited onto nanostructured Si substrates via low-cost thermal evaporation method. Then, the films were annealed in a furnace at temperatures ranging from 400 °C to 1000 °C resulting in crystal growth of the SiGe layers. In general, the annealing temperature for polycrystalline SiGe is between 600 °C – 800 °C. The crystalline structure of the SiGe layer is improved as a function of increased temperature. This is shown by the low FWHM of about 5.27 as compared to the commercially available Ge substrates where the FWHM value is about 5.06. This method also produces more relax Ge layer where the strain value is 0.261.

Keywords: polycrystalline, silicon germanium, thin film, silicon nanostructures, photovoltaic

1. INTRODUCTION

Silicon has historically been the backbone of the photovoltaic industries for decades. It is perhaps the most extensively studied element of the periodic table, well known for its stability and non-toxicity. Defect free Si can be easily grown in either crystalline or amorphous form. Despite all its advantages, Si is hardly an ideal semiconductor material in comparison with other III - V compounds semiconductors such as gallium arsenide (GaAs), or indium phosphide (InP), or even Ge. With low carrier mobility for both electrons and holes as well as limited maximum velocity of about 1 x 10^7 cm/s, Si is considered as "slow" semiconductor [1].

The International Technology Roadmap for Semiconductors (ITRS) report for the year 2013 had identified Ge and $Si_{1-x}Ge_x$ as one of the semiconductors able to improve the performance of Si either as an active layer or substrates for epitaxial growth of group III-IV materials [2]. With high carrier mobility for both holes and electron, Ge is highly desirable in high frequency and high-speed devices. In comparison with Si, the bandgap for Ge is significantly lower; therefore, it operates at lower voltage.

* ayuwazira@unimap.edu.my

Polycrystalline SiGe has attracted the attention of many researchers in photovoltaic devices due to its high efficiency and low production cost [3, 4]. Additionally, control on the electrical and optical properties of the polycrystalline SiGe is possible by tuning its composition [5]. Previous study reported that higher efficiency was possible for SiGe based solar cells compared to polycrystalline Si [6].

In this paper, a simple method to grow the polycrystalline SiGe on high aspect ratio, nanoscale patterned Si substrates is discussed. Instead of lithography and RIE methods for creating nanostructures, a simple yet practical chemical etching method applicable to large areas has been chosen. This method significantly reduces the cost while retaining the ability to reproduce the comparable high quality and high aspect ratio structures to serve as templates for crystal growth. Growth of the polycrystalline SiGe films was subsequently carried out in two steps; the first step was vacuum thermal evaporation of a-Ge films with controllable thickness and the second step was amorphous to crystallization transition as a function of temperature in controlled environments. The proposed technical approach, therefore, eliminates expensive nano-scale patterning and toxic-gas based processing.

2. MATERIAL AND METHODS

Prior to the growth of the SiGe thin films, the Si substrates were synthesis to form nano-pillars structures using the metal assisted chemical etching (MACE) process with Ag as the catalyst. The method to synthesize the nano-pillars were discuss elsewhere [7, 8]. Boron doped, p-type (100) Si substrates with resistivity of 1 – 10 Ω cm range and thickness of 200 µm were used in this process. Following optimized synthesis of Si nano-pillars, growth of Ge films was initiated by means of depositing amorphous films through thermal evaporation technique. The a-Ge films were deposited in a HHV Auto 306 thermal evaporators at vacuum pressure of 5.3 x 10^{-5} Torr, filament current in 6-7A range, and evaporation times in 5 to 10 second range. Ge targets of 99.999 % purity (obtained from RD Mathis) ranging in weight from 500 to 1500 mg were used as sources for deposition, resulting in varying thickness of Ge layers.

Thermal annealing was then conducted for samples deposited with 1.0 mg Ge in a high temperature quartz furnace; an N_2 flow was maintained during heating for time interval of 30 minutes. Four different temperature variations were selected i.e., 400 °C, 600 °C, 800 °C and 1000 °C. The thermal annealing led to recrystallization of the a-Ge films; temperature variation allows accurate determination of film quality as a function of temperature. The samples were then characterized to determine the morphological and optical characteristics using Field Emission Scanning Electron Microscopy (FE-SEM), Raman spectroscopy and X-Ray diffraction (XRD) measurement.

3. RESULTS AND DISCUSSION

Field Emission Scanning Electron Microscopy (FE-SEM) had been used extensively to determine the morphology and thickness of the as-deposited a-Ge films. Study by Chen et al., had demonstrated that thermal annealing was able to improve crystallinity as well as conductivity of SiGe layers [9]. Thermally evaporated Ge films, deposited on patterned Si surfaces were placed in an oven and annealed at 400 °C for 30 minutes in N_2 ambient. Figure 1 (a & b) shows the FE-SEM micrographs of the as deposited and annealed Ge deposited on nanostructured substrates respectively. From these FE-SEM images, minor yet significant changes in the morphology of the as-deposited amorphous layer of Ge can be detected. Although the overall structure remains similar, the annealing process has initiated surface smoothening and volume reduction (Figure 1

(b)). Closer inspection on the top surface of the Ge layer also suggests small scale rounding of as-deposited features as well as absence of any cracks due to thermal expansion mismatch with underlying Si substrate (Figure 1(b(ii))).

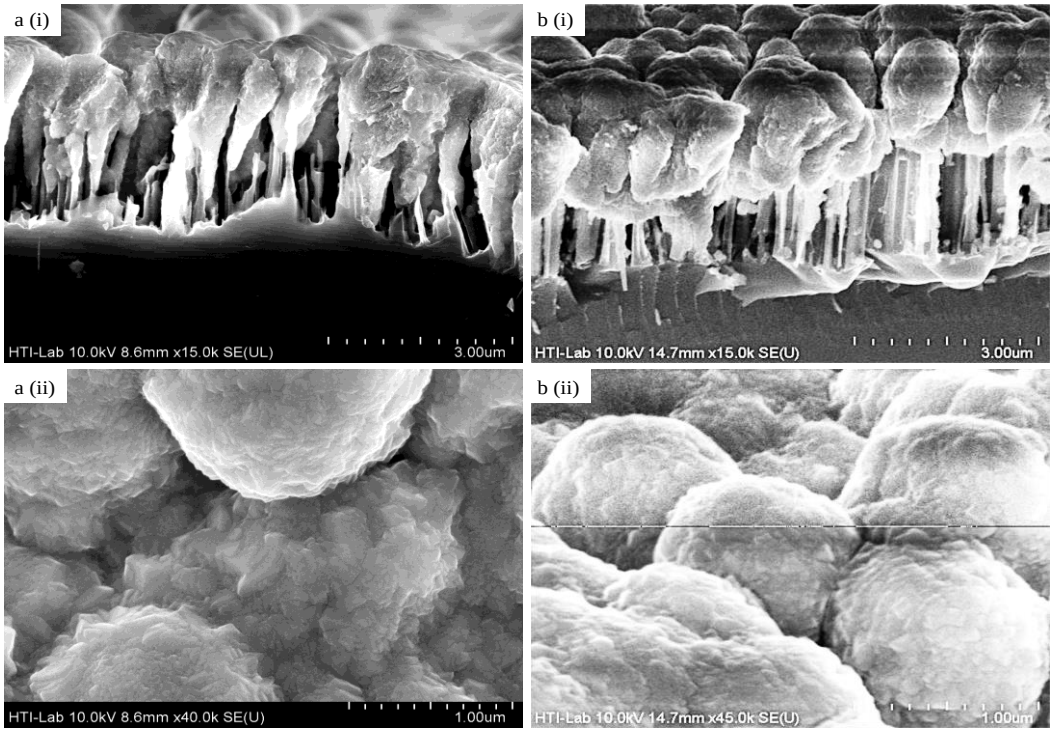

Figure 1. FE-SEM images of (a) as-deposited and (b) 400 °C annealed a-Ge deposited on Si nano-pillars substrates.

This result is consistent with reported study by [10, 11] where no significant morphological changes are observed after annealing at 400 °C. Although other researchers had proposed that recrystallization of a-Ge can occur at annealing temperature of as low as 300 °C [12], this was difficult to quantify with FE-SEM or EDX measurements and will require more sensitive methods based on Raman or XRD analysis. The data in Figure 1 (b) shows that at 400 °C annealing temperature, the process of crystallization has initiated although the effect is difficult to quantify. Most studies indicate that higher degree of crystallinity was achieved at significantly higher temperatures [12, 13].

Additional investigation was carried out using EDX to determine any changes in the Si and Ge content of the annealed structures. Figure 2 (a & b) shows the EDX micrograph of annealed Ge at two different locations representing the top surface of the a-Ge and the Si nano-pillars area of the sample respectively. As predicted, high Ge content is observed at the top surface (67 %) while no Si can be detected. The percentage of O observed is quite high (30 %) while only traces of C is presence believed to be attributed from the carbon tape used as adhesive. At the Si nano-pillars area (Figure 2 (b)), the Ge content reduces significantly to only 15 % while Si content is increase to 22 %. The O content reduces to only 13 % although in terms of its ratio to Ge, it appears that ratio of Ge to O is the same at both top and cross-sectional regions. The presence of high O content may be attributed to formation of SiGe type oxide structure.

To evaluate the amorphous to epitaxial growth, annealing temperature was increased to 700 °C. Figure 3 (a & b) illustrates the cross-sectional and top surface views of the as deposited and

annealed Ge films at 700 °C for 30 minutes. FE-SEM images show that following 700 °C anneal, the a-Ge layer has recrystallized, become smoother, with significant growth on the sidewalls of the Si nano-pillars. It is also observed that the a-Ge films at the top of the Si nano-pillars tend to coalesce to form crystalline Ge islands [11]. Smoother surface of the Ge layer is also noticed for the annealed samples. Most reported work agrees that the growth of crystalline Ge structures is achieved at temperatures in 600 °C to 700 °C range [14, 15].

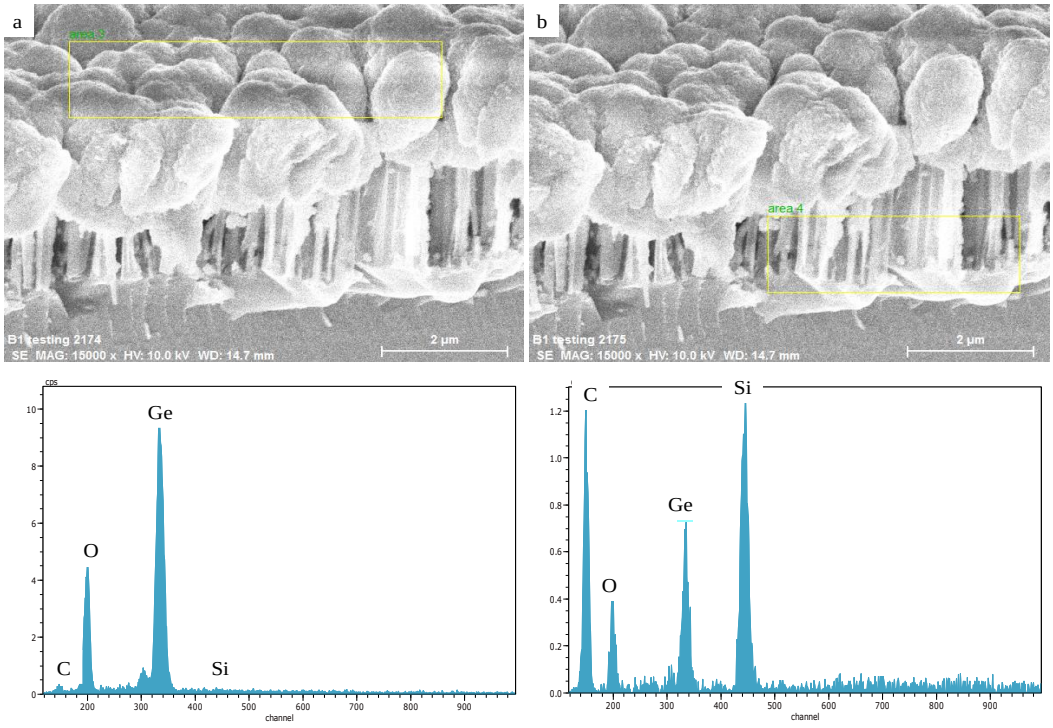

Figure 2. EDX analysis for Ge deposited on nano-pillars substrates. Two different locations are chosen representing (a) the top Ge surface and (b) cross-sectional area of the Si nano-pillars area.

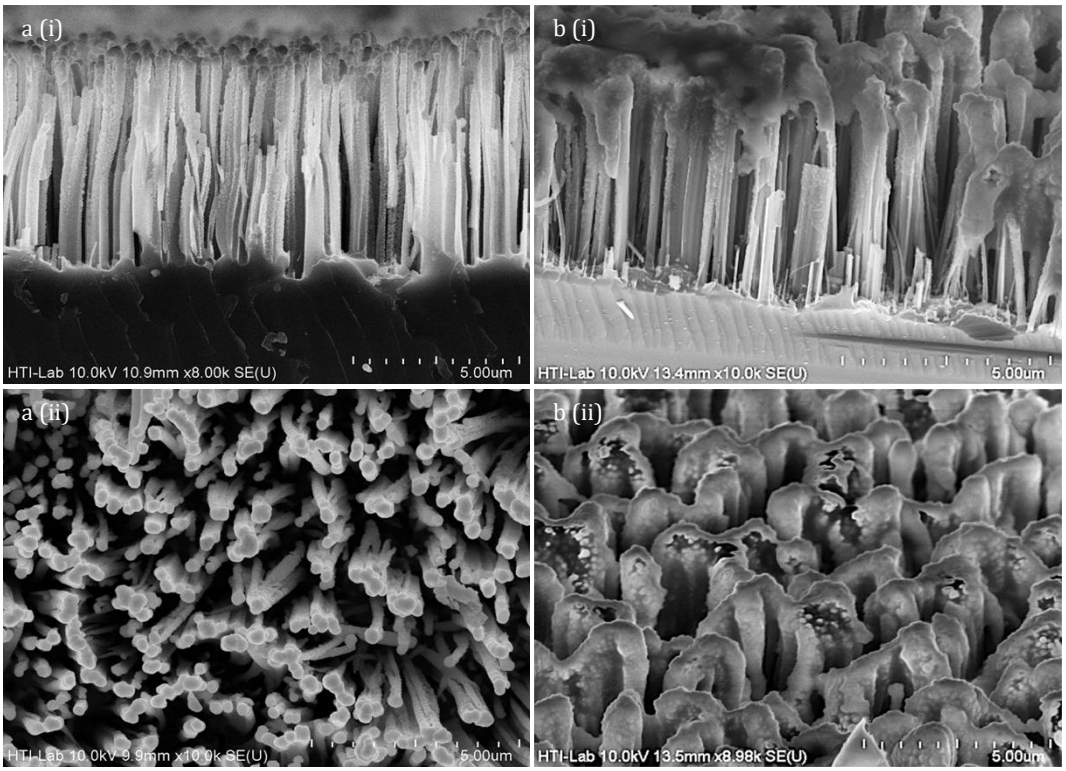

Figure 3. FE-SEM images of (a) as-deposited and (b) 700 °C annealed a-Ge deposited on Si nano-pillars substrates.

An EDX analysis was carried out to evaluate changes in Ge and Si content of the annealed samples. Figure 4 shows the EDX analysis of annealed Ge films at (a) top surface area and (b) cross-sectional nano-pillars area. High concentrations of C and O are observed at the top Ge surface. However, only traces of these elements are detected at the cross-sectional nano-pillar area. As seen earlier for 400 °C anneal, the ratios of Ge to O are similar at the top surface. One large difference relative to 400 °C anneal is the significant (7 %) detection of Si. This may be attributed due to volume reduction from amorphous to crystalline phase to allow higher x-ray transmission through the Ge film resulting in Si measurement. EDX analysis around the vicinity of the Si nano-pillars shows significant reduction in Ge, O and C with similar ratios of Ge to O; high Si content is observed at almost 75 %.

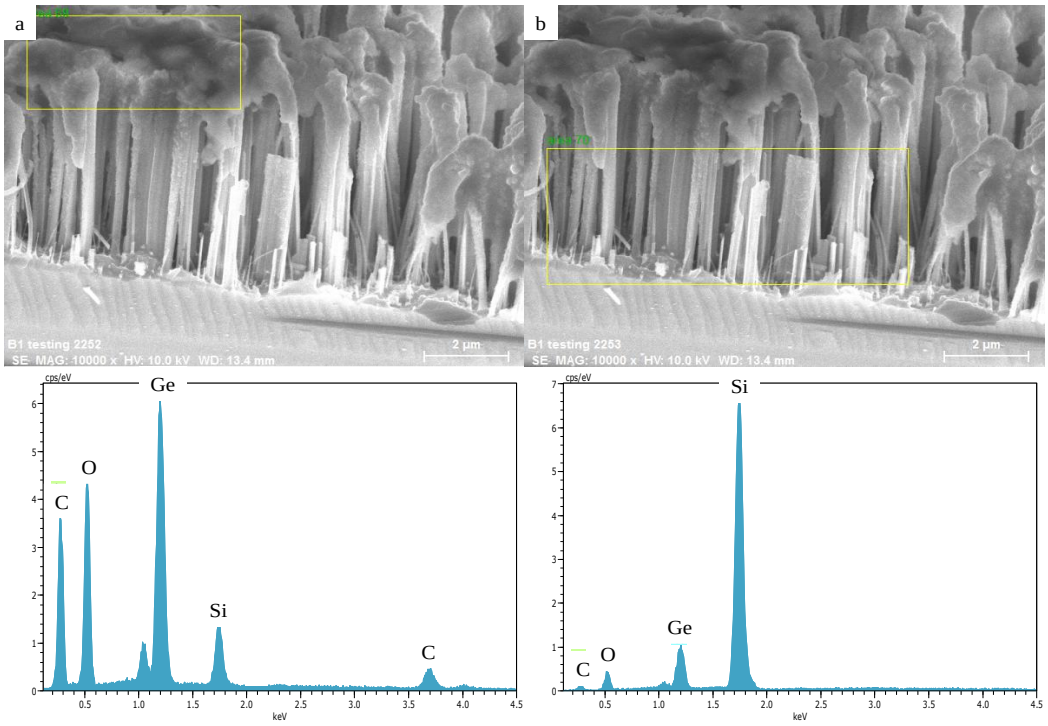

Figure 4. EDX analysis for annealed Ge deposited on nano-pillars substrates at (a) the surface area and (b) nano-pillars area; the annealing temperature was 700 °C.

Figure 5 illustrates the (i) top and (ii) cross-sectional images of a-Ge films after thermal annealing at 1000 °C. Annealing at 1000 °C, leads to low density of cracks with films growing epitaxially around respective nano-pillars. It is also noticeable that the Si nano-pillars profiles remain intact during Ge epitaxial growth process. Top view exhibits islands of clustered Ge with minor cracks present but at reduced extent.

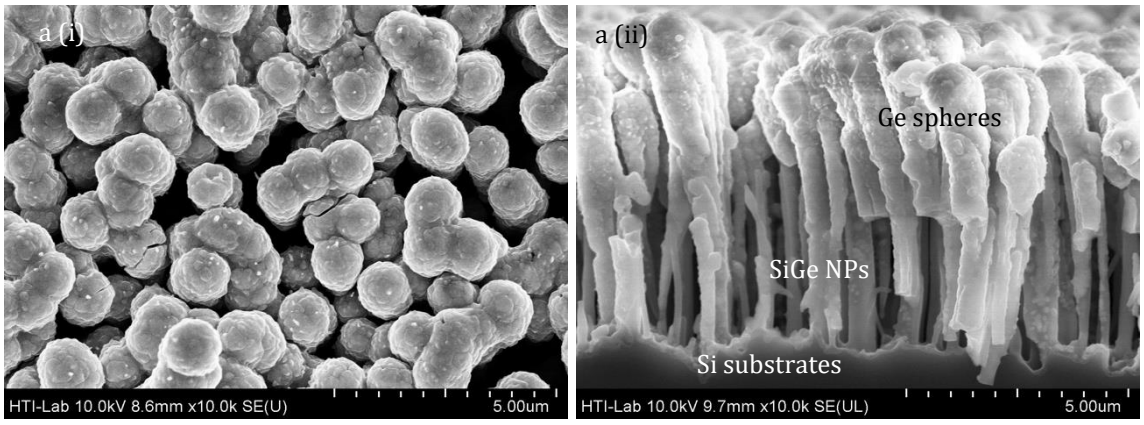

Figure 5. (i) Top-view and (ii) cross-sectional FE-SEM images of thermally annealed a-Ge films.

EDX analysis of the annealed Ge film is presented in **Figure 6**. Consistent with earlier results, the top surface ratios of Ge to oxygen are consistent with the formation of SiGe film . In the cross-sectional region representing a mixture of Ge and nano-pillars, the concentration of Si is highest,

followed by O and Ge. Higher O concentration can be related to native oxides of both Ge and Si. The concentrations of Ge and O are negligible in the substrate region.

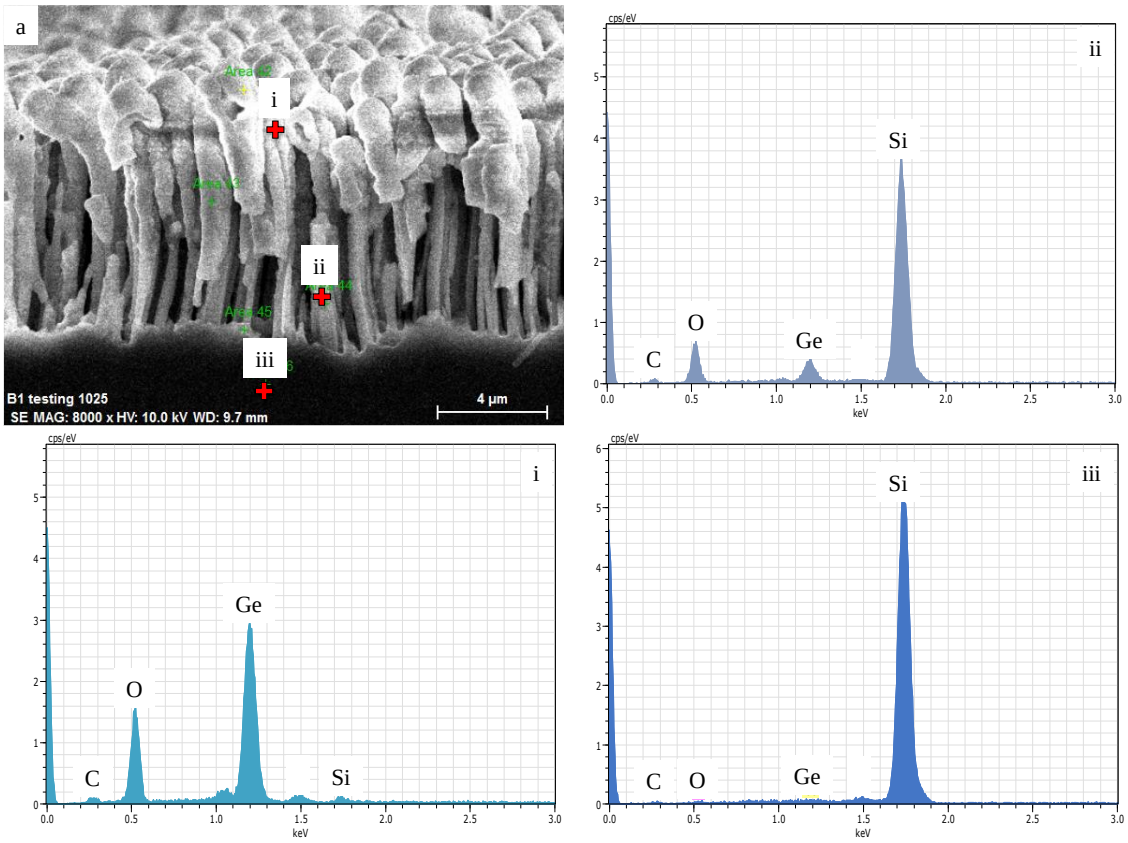

Figure 6. EDX analysis for annealed Ge at 1000 °C. Three different locations are chosen representing: (i) Ge surface, (ii) Si cross-sectional nano-pillar region and (iii) Si substrate.

Additional confirmation of high-quality oxide formation in crystalline Ge films is evident in relative comparison of EDX data in Figure 7. As-deposited Ge films exhibit Ge to O concentration ratio of almost 4 (Figure 7(a)), i.e., O concentration is factor of 4 lower than Ge. Following annealing, ratio of Ge to O concentration is reduced approximately by a factor of 2, i.e., O concentration has increased by factor of 2 (Figure 7 (b)). However, the percentage of Si does not differ as much before and after being subjected to thermal annealing due to sufficient film thickness and uniformity. It is possible to eliminate oxide formation by carrying out annealing process in vacuum.

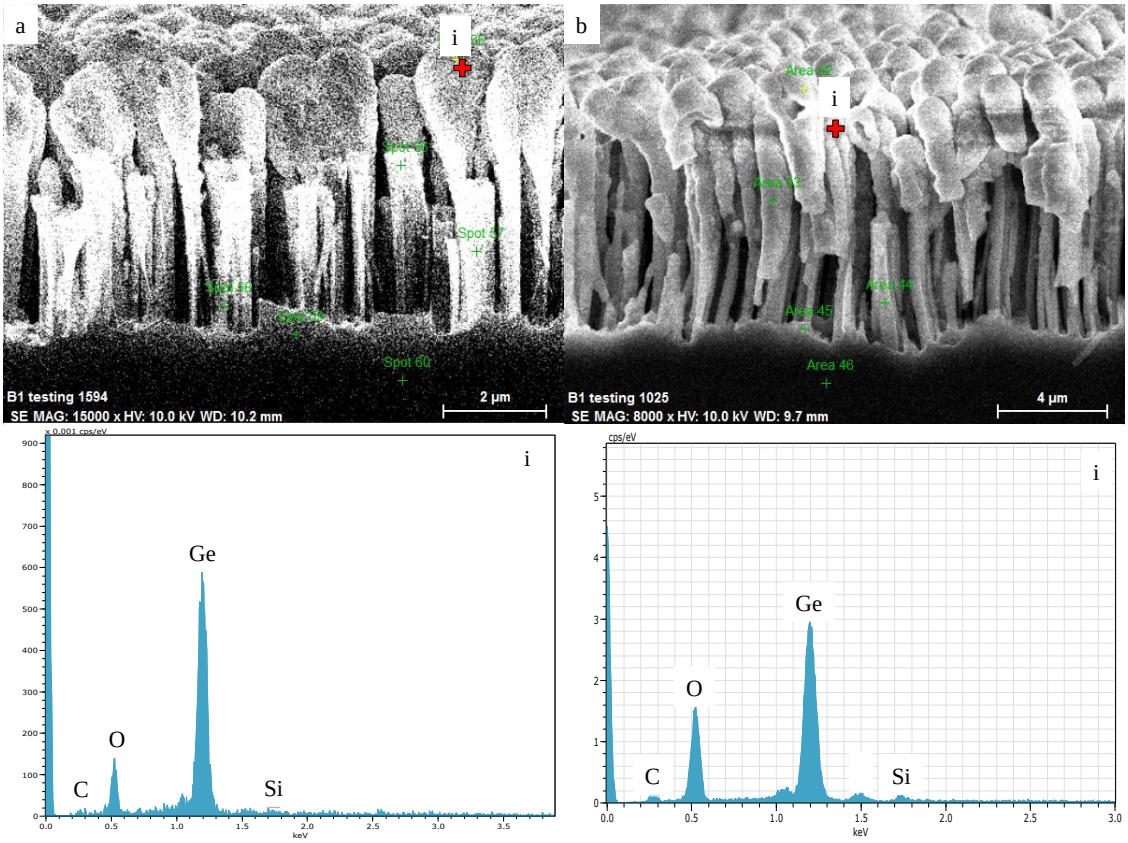

Figure 7. Comparison between (a) as-deposited Ge films and (b) annealed Ge films

Figure 8 illustrates how annealing of different thicknesses of a-Ge thin films deposited on nano-pillars substrates leads to recrystallization of the Ge films on top and sidewalls of the Si nano-pillars and coalescence of crystalline layers on adjacent nano-pillars. For thin films (Figure 8(a)), surface cracks due to thermal expansion mismatch could not be observed. However, as film thickness is increased (Figure 8(b) & (c)), cracks in the crystalline layer started to emerge. At the thickest film (Figure 8(c)), higher density of surface cracks is observed. Another interesting observation relates to the coalescence between adjacent Si nano-pillars is the formation of smooth crystalline Ge films.

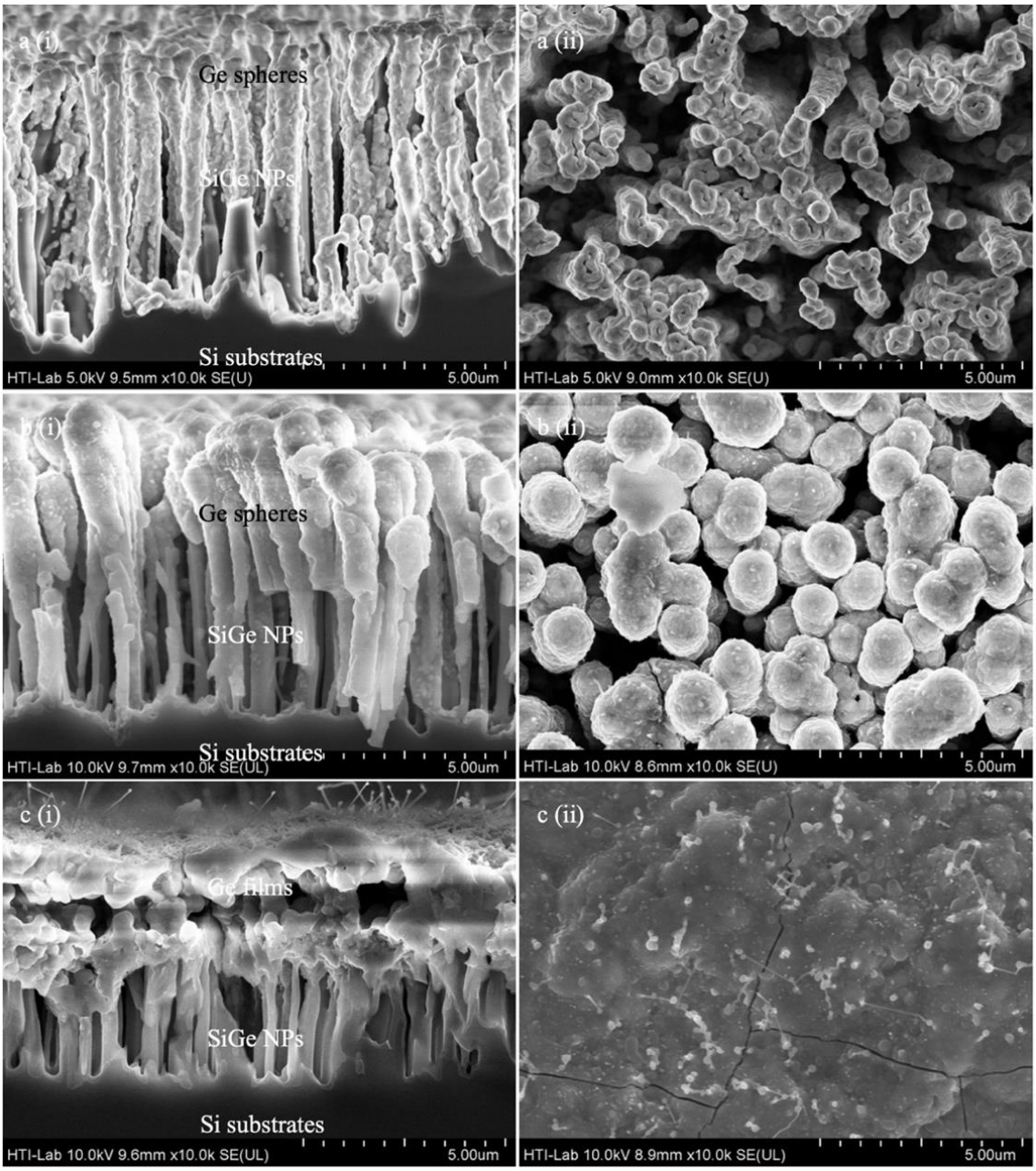

Figure 8. (i) Cross-sectional and (ii) top-view FE-SEM images of crystalline Ge films grown on nano-pillars surfaces after annealing at 1000°C for different a-Ge thicknesses (by weight): (a) 0.5 mg, (b) 1.0 mg, and (c) 1.5 mg.

Structural evolution of vacuum-evaporated a-Ge and thermally annealed crystalline Ge films had been investigated with Raman spectroscopy. Figure 9 plots the Raman spectra measured from polished Si and Ge wafers to serve as baseline references. Two dominant peaks were identified; the Ge-Ge peak at 300 cm^{-1} and the Si-Si peak centered at 520 cm^{-1}. The FWHM for both peaks are measured at 4.69 cm^{-1} and 5.06 cm^{-1} for the Si-Si peak and Ge-Ge peak respectively.

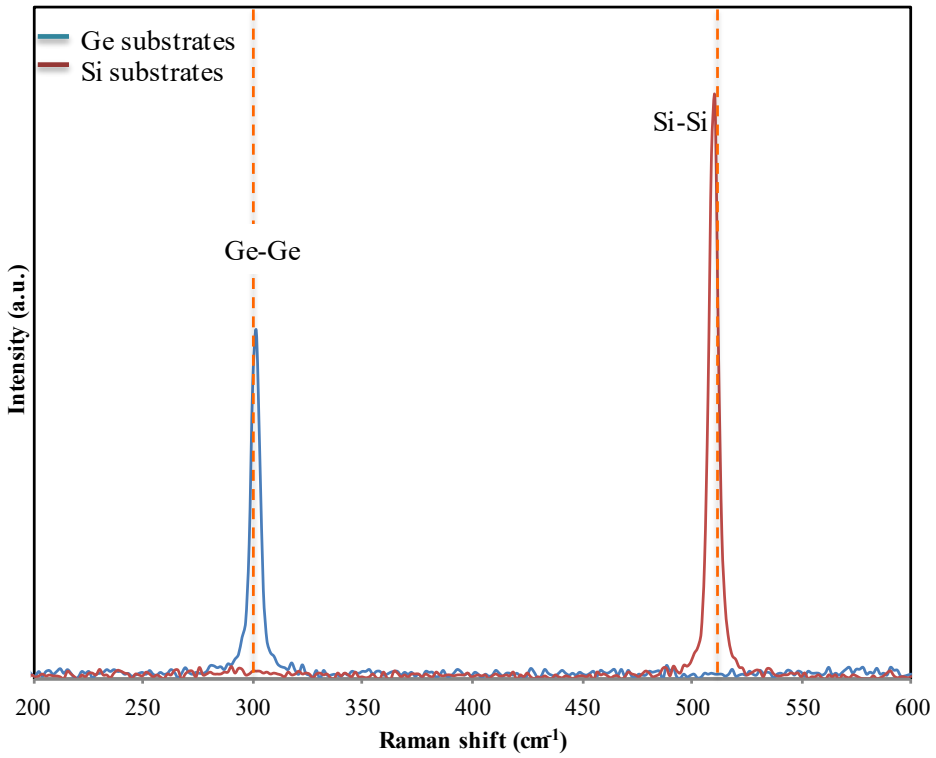

Figure 9. Measured Raman spectra from crystalline Si and Ge substrates.

Detailed Raman scattering measurements of annealed Ge films at different thicknesses (measured by weight; 0.5 g, 1.0 g and 1.5 g Ge) and temperatures (400 °C, 600 °C, 800 °C and 1000 °C) are presented in order to establish correlations between film quality and surface structure. Raman scattering spectra of annealed Ge deposited on nano-structured Si surfaces with three different thicknesses has been plotted in Figure 10. From the Raman spectra, three major peaks are visible at around 290 cm^{-1}, 445 cm^{-1} and 520 cm^{-1} representing the Ge-Ge peak, Si-Ge peak, and Si-Si peak respectively. The Raman spectra exhibit increase in the peak intensity of both the Si-Ge and Ge-Ge peaks as a function of the increase in the thickness of the deposited Ge film. For deposition on nano-pillars substrates, the Ge-Ge Raman peak for thin Ge films (0.5 mg and 1.0 mg Ge) is less visible compared to the thick Ge films (1.5 mg Ge). To determine the crystalline quality of various films thickness, the FWHM of each peak were measured. Table 1 summarizes the FWHM of the Ge-Ge and Si-Ge peaks at various Ge films thickness. The FWHM values show increment for both the Si-Ge and Ge-Ge peaks as a function of the increase in the thickness of the deposited Ge film. However, the FWHM of Ge-Ge peak for 0.5 g Ge deposited cannot be quantified.

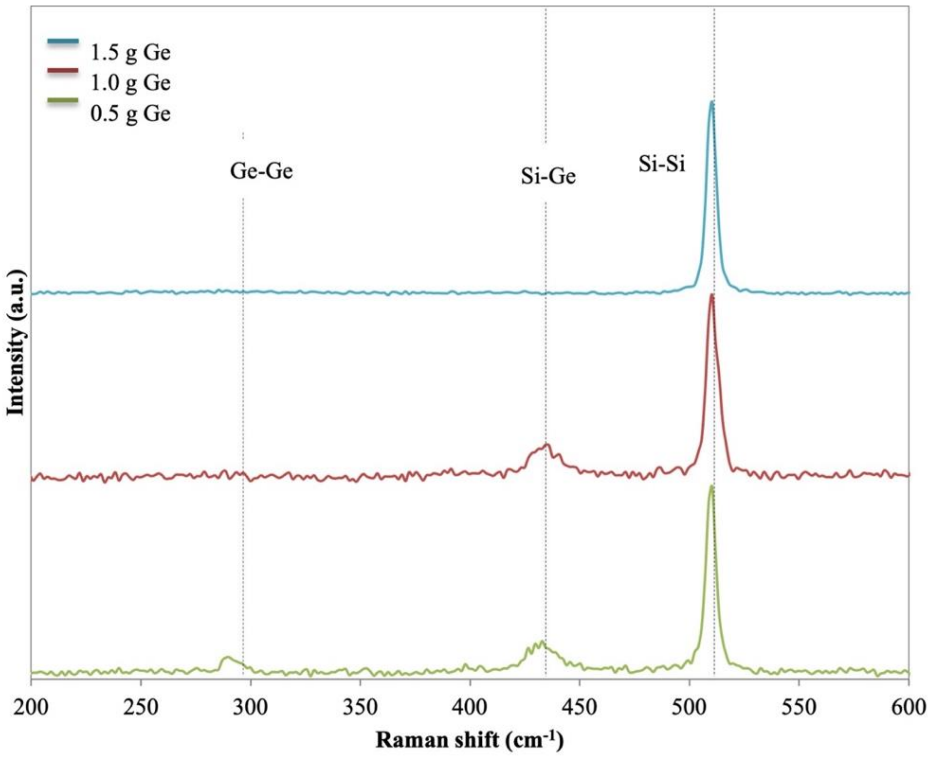

Figure 10. Raman spectra of annealed Ge deposited on nano-pillars substrates at various thicknesses (measured by weight) namely 0.5 g, 1.0 g and 1.5 g Ge.

Table 1. Measured FWHM of the Ge-Ge peak and Si-Ge peak for various thickness of Ge deposited on nano-pillars Si substrates.

Ge thickness (weight)	FWHM (cm^{-1}) (Ge-Ge peak)	Peak location (cm^{-1})	FWHM (cm^{-1}) (Si-Ge peak)	Peak location (cm^{-1})
0.5 g	-	-	14.45	433.23
1.0 g	14.08	291.89	16.28	433.06
1.5 g	15.04	289.75	17.34	432.88

Figure 11 plots the Raman spectra of a-Ge films annealed at temperatures in 400 °C to 1000 °C range; all films were deposited on nano-pillars substrates. The inset in **Error! Reference source not found.** illustrates Raman spectra ranging from 200 cm^{-1} to 500 cm^{-1} to provide a better view of the Ge-Ge and Si-Ge peaks. From the Raman spectra, the presence of strong amorphous Ge-Ge peak and weak Si-Ge and Si-Si peaks are observed, indicating lack of crystallization at 400 °C. the emergence of strong and symmetric Ge-Ge peak cantered at 297 cm^{-1} following 600 °C temperature anneals suggesting transition from amorphous to crystalline phase. This is accompanied by quenching of Si-Ge peak and the emergence of Si-Si peak at 520 cm^{-1}.

Continued high frequency shift of the Ge-Ge peak with higher intensity following thermal annealing at 800 °C signifying further improvement in the crystallinity of the Ge layer where slight increase in Si-Ge peak is also noticeable. Finally, it is observed that the strong Ge-Ge peak is replaced by a weak and broad Ge-Ge & Si-Ge peaks following annealing at 1000 °C. The significant change detected for annealing at 1000 °C suggests that the a-Ge film recrystallizes to random arrangements of the particles that lead to the formation of the amorphous like humps [16]. A

slight shift towards the high frequency as a function of temperature is indicative of decreases of the compressive strain in the Ge layer towards relaxation [13, 17] and increase in the composition of Ge [18]. On the other hand, the shift towards smaller wave number is due to tensile strain [19].

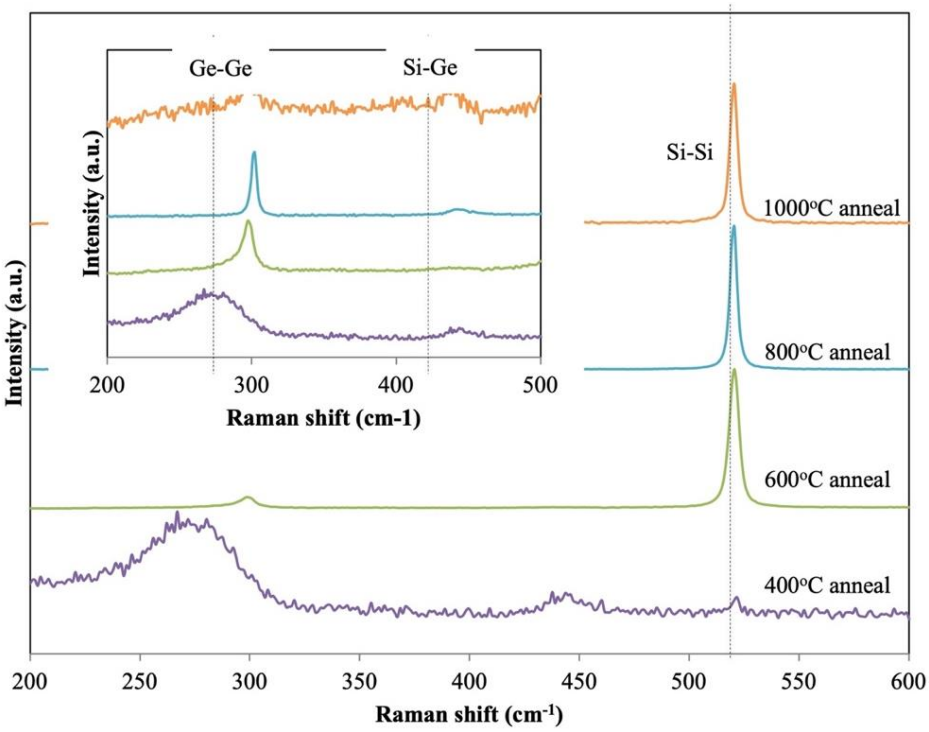

Figure 11. Raman spectra of thermally annealed Ge films deposited nano-pillars substrates at various annealing temperature.

The crystalline qualities of the Ge films are quantified by measuring the FWHM values for each peak and are shown in Table 2. From the FWHM values, it can be concluded that the crystalline quality of the Ge films increases with temperature. This is shown by the reduction in the FWHM values from 57.13 cm^{-1} for annealing at 400 °C to 8.91 cm^{-1} and 5.27 cm^{-1} for annealing at 600 °C and 800 °C respectively. The low FWHM value for Ge films annealed at 800 °C shows an almost perfect crystalline structure where the FWHM for crystalline Ge is measured at 5.06 cm^{-1}. However, for annealing at 1000 °C, the broad peak resulted in high FWHM value i.e., 14.08 cm^{-1}. As for the Si-Ge peak, identical results are replicated where the increasing annealing temperature leads to improvement in the crystalline structure, hence the reduction in the FWHM values.

Table 2. Measured FWHM of the Ge-Ge peak and Si-Ge peak for various annealing temperature of Ge deposited on nano-pillars Si substrates.

Annealing temperature (˚C)	FWHM (cm^{-1}) (Ge-Ge peak)	Peak location (cm^{-1})	FWHM (cm^{-1}) (Si-Ge peak)	Peak location (cm^{-1})
400	57.13	269.5	22.02	445.7
600	8.91	298.4	-	-
800	5.27	301.6	16.48	444.2
1000	14.08	291.89	16.28	433.06

X-ray diffraction (XRD) is often used to measure the strain, crystallite size, and crystallinity of the thin and bulk substrates. Although a high resolution XRD is preferably used to characterize the growth of a-Ge films, in this study, a powder XRD measurement system is used instead. This is because powder XRD system has sufficient resolution to provide detail measurements of the strain, crystallite size, and crystallinity of the Ge films on Si. From the XRD spectra, in can be concluded that thermal-annealing of a-Ge films causes epitaxial crystalline growth leading to polycrystalline Ge structures identified by the multiple Ge peaks in the XRD spectra [12]. A single peak is present if the crystalline structures are in single crystal forms [20]. The peak intensity exhibits noticeable increase with annealing suggesting closer atomic position for both Si and Ge [15].

Figure 12 plots the XRD spectrum for as deposited and annealed Ge films deposited on nano-pillars substrates. Annealing was conducted at four different temperatures: from 400 °C to 1000 °C. From the XRD spectra, polycrystalline SiGe structures with major peaks at (100), (101), (012) and (200) planes were observed. This is supported by a symmetric Ge-Ge peak identified in the Raman spectra (Figure 11) [21-23]. The same identical peaks are also visible for the annealed samples. It is also observed that the maximum peak intensity for all samples is centered on the (101) plane with increased intensity as a function of temperature. For Ge films annealed at 800 °C and 1000 °C, a slight peak is observed corresponding to the Ge (220) planes [24]. It is likely that crystalline growth initiates at the interface between the deposited Ge layer and the nano-pillars substrate during the initial growth of Ge but is not detected by the Raman spectroscopy [20]. In fact, most studies agrees that recrystallization of Ge starts at annealing temperature of as low as 250 °C and the crystal quality is improved with increasing temperature [25, 26].

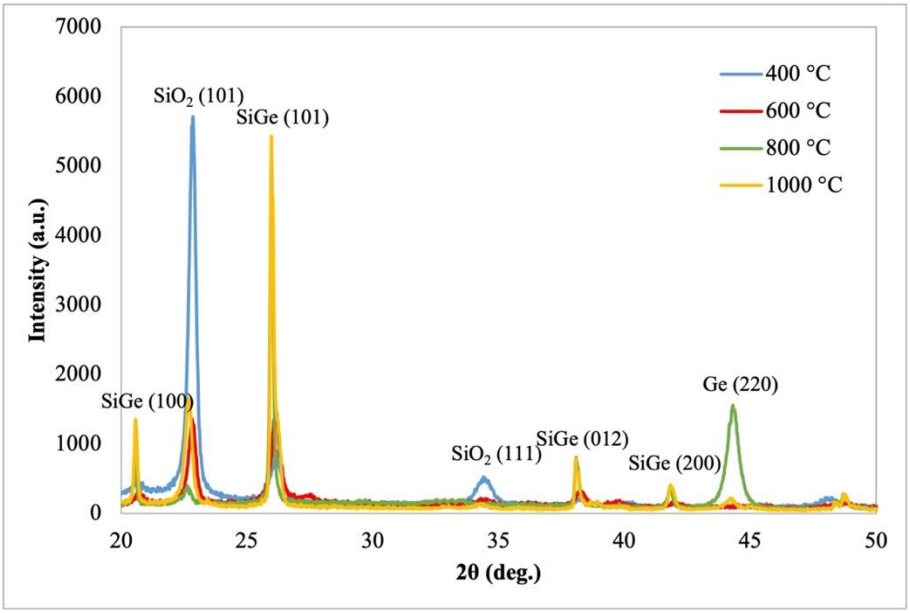

Figure 12. X-ray diffraction pattern of a-Ge films deposited on nano-pillars substrates and annealed at various annealing conditions.

The lattice parameter of the samples is presented in Table 3. From the FWHM value it is obvious that the crystal quality is improved when annealing is conducted above 600 °C as seen by the reduction in the FWHM from 0.236 ° to less than 0.138 ° for all samples annealed at 800 °C and above [12]. This is consistent with the measurement by Raman spectroscopy where a more prominent Raman peak is visible when annealing is conducted at temperature of 800 °C (**Error!**

Reference source not found.). XRD measurement revealed polycrystalline Ge and SiGe nanostructures with tetragonal phases. This result is in line with another study by Abd Rahim et al. where in their study, polycrystalline Ge with tetragonal Ge phases was observed when a-Ge was annealed [10].

Table 3. Peak position, FWHM, lattice constant, crystallite size and strain variation with annealing for SiGe (101) plane.

Sample	Peak position (2θ)	FWHM (2θ)	Lattice parameter			Crystallite size (Å)	Strain (%)
			a (Å)	b (Å)	c (Å)		
400 °C	26.126	0.236	4.947	4.947	5.625	346	0.444
600 °C	25.955	0.236	4.986	4.986	5.647	346	0.447
800 °C	25.955	0.138	4.986	4.986	5.647	591	0.261
1000 °C	25.956	0.138	4.985	4.985	5.648	591	0.261

4. CONCLUSION

Morphological and optical study of the amorphous and annealed Ge films deposited at different thickness and annealing temperature were carried out to determine the crystalline quality of the Ge films. From the FESEM analysis, it can be concluded that the film thickness for deposition on nano-pillars substrates was hard to quantify due to the non-conformal deposition of the Ge films. However, it was observed that for deposition of thin layer of a-Ge, islanding of the films occurs attributed to the isotropic nature of deposition process. Increased films thickness causes coalescence of a-Ge films halfway through the middle part of the Si nano-pillars due to the high aspect ratio. For deposition below 1.0 g (by weight), no formation of cracks was observed believed to be due to discontinuities nature of the films.

Annealing was conducted for recrystallization of the a-Ge films at various annealing temperature ranging from 400 °C to 1000 °C. Optical characterization of the samples provided better insight of the a-Ge films before and after annealing. When subjected to thermal annealing, different behaviors were observed for all samples indicating transformation of the a-Ge films towards crystal structure. Inspection of the crystalline quality of annealed Ge films with different thickness showed that the crystalline quality decreases with the increase in thickness as can be perceived by the increased FWHM values for both Ge-Ge and Si-Ge peaks. This may be due to several reasons. For instance, thick Ge films results in slow recrystallization process, hence broader FWHM values were measured.

When subjected to various annealing temperature, crystalline quality of the Ge films showed improvement as a function of increasing temperature as can be observed from the Raman FWHM measurement. However, when the annealing temperature reached 1000 °C, broader peak was observed believe to be attributed to the random arrangement of the particles. The optimum annealing temperature is believed to be at 800 °C. This was confirmed by the measurement of the FWHM of about 5.27 cm^{-1}, which was almost identical to the FWHM value of a perfect crystalline Ge of about 5.06 cm^{-1}. Comparison of the FWHM value between the thermal annealed samples with Ge substrates at 800 °C is as depicted in Figure 13. The Ge-Ge peak clearly shows that the broadening of the sample is almost the same size as the Ge substrates as shown in Figure 13 (a). The Si-Ge peak is obviously not present for the Ge substrates but is existed for the thermal

annealed samples as shown in Figure 13 (b). This value is in fact very low as compared to another similar study by Abd. Rahim et al. where the lowest FWHM value that was achieved in that study was 13.28 at the annealing temperature of 700 °C [10].

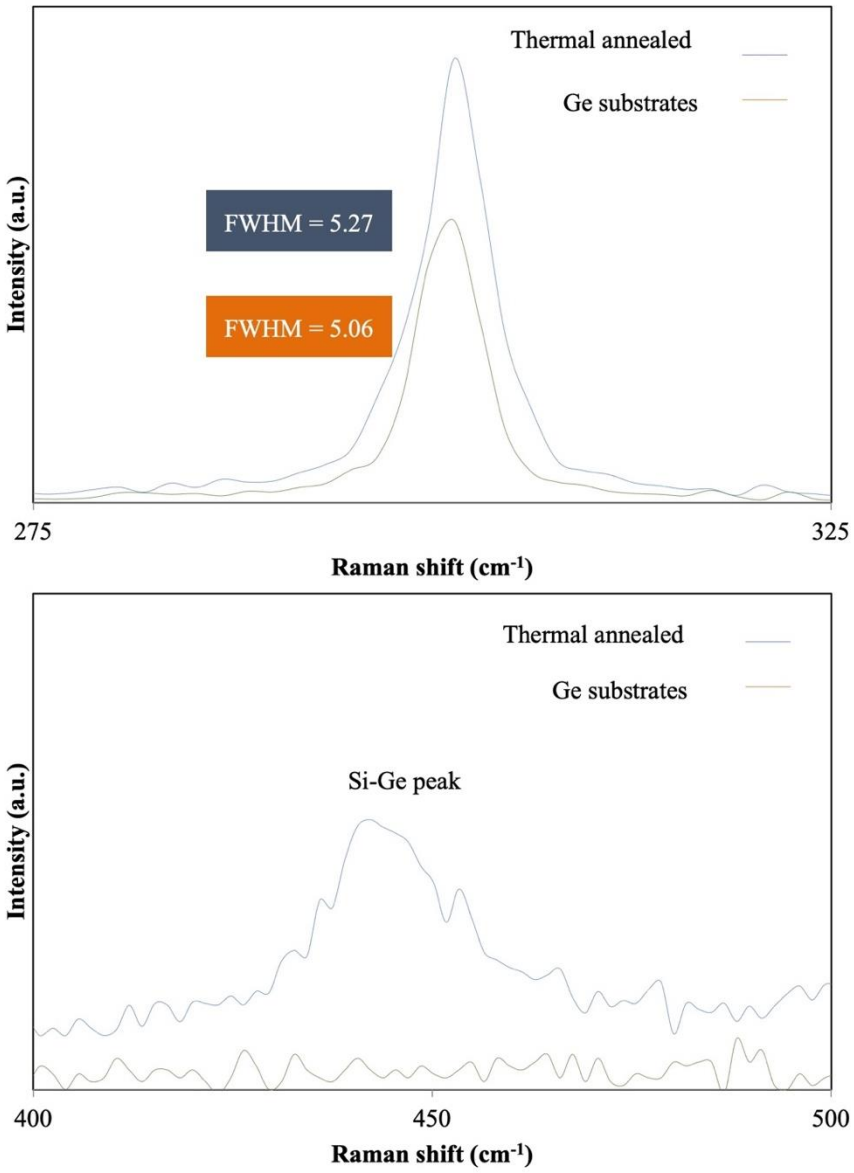

Figure 13. Comparison of the FWHM values between the thermal annealed samples and Ge substrates. Top: Shows the Ge-Ge peak of the samples and Bottom: shows the Si-Ge peak of the samples.

The improved crystalline qualities of the Ge films as a function of temperature were also quantified using XRD measurement. Results showed were identical to those of Raman analysis. Major peaks were observed corresponding to the SiGe (101) and SiO_2 (101) planes. In addition, minor peaks were also observed corresponding to the SiGe (100), (012) and (200) planes. The XRD peak for thermal annealed samples is presented in **Error! Reference source not found.**. As can be seen from this figure, the SiGe peak was prominent for the SiGe (100) and (101) planes. XRD analysis on the strain showed reduction in the strain value as annealing temperature was increased. In this study, the lowest strain was 0.261 % for annealing at 800 °C and 1000 °C. The

strain value showed in this study was lower as compared to another study by Abd Rahim et al. where in his study the lowest strain was 0.54 % [10]. Lower strain value is very much favorable in most electronic application such as in transistor as it indicated more relax layer. Hence in this study, it could be conclude that for annealing at 800 °C the Ge and SiGe was becoming more relaxed [27].

ACKNOWLEDGEMENTS

The author would like to acknowledge the support from the Fundamental Research Grant Scheme (FRGS) under a grant number of ***FRGS/1/2017/TK07/UNIMAP/02/1*** from the **Ministry of Higher Education Malaysia**

REFERENCES

[1] J. D. CresslerG. Niu, Silicon-Germanium Heterojunction Bipolar Transistors, Ed. Noorwood, MA: Arctech House, Inc, (2003) pp.
[2] ITRS, International Technology Roadmap for Semiconductors International Technology Roadmap for Semiconductors, (2013)
[3] A. Ali, S. L. Cheow, A. W. Azhari, K. SopianS. H. Zaidi, Results in Physics vol **7**, (2017) pp. 225-232.
[4] Sige: A Key to Unlocking the Potential of Solar Cells, (2003) pp. 7-9.
[5] W. Pan, K. Fujiwara, N. Usami, T. Ujihara, K. NakajimaR. Shimokawa, Journal of Applied Physics vol **96**, issue 2 (2004) pp. 1238-1241.
[6] K. Nakajima, N. Usami, K. Fujiwara, Y. Murakami, T. Ujihara, G. SazakiT. Shishido, Solar Energy Materials and Solar Cells vol **72**, issue 1 (2002) pp. 93-100.
[7] A. W. Azhari, B. T. Goh, S. Sepeai, M. Khairunaz, K. SopianS. H. Zaidi., "Synthesis and Characterization of Self-Assembled, High Aspect Ratio Nm-Scale Columnar Silicon Structures," in 39th IEEE Photovoltaic Specialists Conference, Tampa, Florida, (2013 of Conference)
[8] A. W. Azhari, K. Sopian, M. K. M. DesaS. H. Zaidi, Applied Surface Science vol **357**, (2015) pp. 1863-1877.
[9] Y.-H. Chen, J.-C. Liu, Y.-R. Chen, J.-W. Lin, C.-H. Chen, W.-H. LuC.-N. Li, Thin Solid Films vol **529**, (2013) pp. 7-9.
[10] A. F. Abd Rahim, M. R. Hashim, N. K. Ali, M. Rusop, M. D. Johan OoiM. Z. M. Yusoff, Applied Surface Science vol **275**, (2013) pp. 193-200.
[11] C. Khare, J. W. Gerlach, T. Höche, B. Fuhrmann, H. S. LeipnerB. Rauschenbach, Applied Surface Science vol **258**, issue 24 (2012) pp. 9762-9769.
[12] R. A. Ismail, O. A. AbdulrazaqJ. Koshaba, Materials Letters vol **60**, issue 19 (2006) pp. 2352-2356.
[13] K. Oda, K. Tani, S.-i. SaitoT. Ido, Thin Solid Films vol **550**, (2014) pp. 509-514.
[14] F. Edelman, Y. Komem, M. Stolze, P. WernerR. Butz, (1996) pp.
[15] A. F. A. Rahim, M. R. Hashim, N. K. Ali, M. Rusop, M. D. J. OoiM. Z. M. Yusoff, Applied Surface Science vol **275**, (2013) pp. 193-200.
[16] W. Choi, Y. HoV. Ng, Mater. Phys. Mech. vol **4**, (2001) pp. 46-50.
[17] B. P. Coonan, N. Griffna, J. T. Beechinor, M. Murtagh, G. Redmond, G. M. Crean, B. HollaÈnder, S. Mantl, S. Bozzo, J.-L. Lazzari, F. A. d'Avitaya, J. DerrienD. J. Paul, Thin Solid Films vol **364**, (2000) pp. 75-79.
[18] K. Jang, Y. Kim, J. ParkJ. Yi, Materials (Basel) vol **12**, issue 11 (2019) pp.
[19] Y. Tan C. Tan, Thin Solid Films vol **520**, issue 7 (2012) pp. 2711-2716.
[20] A. SuzukiM. Isomura, Journal of Non-Crystalline Solids vol **358**, issue 17 (2012) pp. 2166-2170.
[21] G. M. D. Grier, North Dakota State University, Journal vol 00-043-1012, issue Issue (1994)
[22] J. D. Jorgensen, Journal of Applied Physics vol **49**, issue 11 (1978) pp. 5473-5478.
[23] J. Glinnemann, H. King Jr, H. Schulz, T. Hahn, S. J. La PlacaF. Dacol, Zeitschrift für Kristallographie-Crystalline Materials vol **198**, issue 1-4 (1992) pp. 177-212.

[24] A. SmakulaJ. Kalnajs, Physical Review vol **99**, issue 6 (1955) pp. 1737.
[25] G. Masini, L. Colace, F. GalluzziG. Assanto, Materials Science and Engineering vol **B 69–70** (2000) pp. 257–226.
[26] V. Sorianello, L. Colace, N. Armani, F. Rossi, C. Ferrari, L. LazzariniG. Assanto, Optical Materials Express vol **1**, issue 5 (2011) pp. 856-865
[27] D. Chrastina, G. Isella, M. Bollani, B. Rössner, E. Müller, T. Hackbarth, E. Wintersberger, Z. Zhong, J. StanglH. von Känel, Journal of Crystal Growth vol **281**, issue 2-4 (2005) pp. 281-289.

International Journal of Nanoelectronics and Materials

In Press, Accepted Manuscript – Note to user